RECOMMENDATION ITU-R P.530-8

PROPAGATION DATA AND PREDICTION METHODS REQUIRED FOR THE DESIGN OF TERRESTRIAL LINE-OF-SIGHT SYSTEMS

(Question ITU-R 204/3)

(1978-1982-1986-1990-1992-1994-1995-1997-1999)

The ITU Radiocommunication Assembly,

considering

a) that for the proper planning of terrestrial line-of-sight systems it is necessary to have appropriate propagation prediction methods and data;

b) that methods have been developed that allow the prediction of some of the most important propagation parameters affecting the planning of terrestrial line-of-sight systems;

c) that as far as possible these methods have been tested against available measured data and have been shown to yield an accuracy that is both compatible with the natural variability of propagation phenomena and adequate for most present applications in system planning,

recommends

1 that the prediction methods and other techniques set out in Annexes 1 and 2 be adopted for planning terrestrial line-of-sight systems in the respective ranges of parameters indicated.

ANNEX 1

1 Introduction

Several propagation effects must be considered in the design of line-of-sight radio-relay systems. These include:

– diffraction fading due to obstruction of the path by terrain obstacles under adverse propagation conditions;

– attenuation due to atmospheric gases;

– fading due to atmospheric multipath or beam spreading (commonly referred to as defocusing) associated with abnormal refractive layers;

– fading due to multipath arising from surface reflection;

– attenuation due to precipitation or solid particles in the atmosphere;

– variation of the angle-of-arrival at the receiver terminal and angle-of-launch at the transmitter terminal due to refraction;

– reduction in cross-polarization discrimination (XPD) in multipath or precipitation conditions;

– signal distortion due to frequency selective fading and delay during multipath propagation.

One purpose of this Annex is to present in concise step-by-step form simple prediction methods for the propagation effects that must be taken into account in the majority of fixed line-of-sight links, together with information on their ranges of validity. Another purpose of this Annex is to present other information and techniques that can be recommended in the planning of terrestrial line-of-sight systems.

Prediction methods based on specific climate and topographical conditions within an administration's territory may be found to have advantages over those contained in this Annex.

With the exception of the interference resulting from reduction in XPD, the Annex deals only with effects on the wanted signal. Some overall allowance is made in § 2.3.5 for the effects of intra-system interference in digital systems, but otherwise the subject is not treated. Other interference aspects are treated in separate Recommendations, namely:

– inter-system interference involving other terrestrial links and earth stations in Recommendation ITU-R P.452,

– inter-system interference involving space stations in Recommendation ITU-R P.619.

To optimize the usability of this Annex in system planning and design, the information is arranged according to the propagation effects that must be considered, rather than to the physical mechanisms causing the different effects.

It should be noted that the term “worst month” used in this Recommendation is equivalent to the term “any month” (see Recommendation ITU-R P.581).

2 Propagation loss

The propagation loss on a terrestrial line-of-sight path relative to the free-space loss (see Recommendation ITU-R P.525) is the sum of different contributions as follows:

– attenuation due to atmospheric gases,

– diffraction fading due to obstruction or partial obstruction of the path,

– fading due to multipath, beam spreading and scintillation,

– attenuation due to variation of the angle-of-arrival/launch,

– attenuation due to precipitation,

– attenuation due to sand and dust storms.

Each of these contributions has its own characteristics as a function of frequency, path length and geographic location. These are described in the paragraphs that follow.

Sometimes propagation enhancement is of interest. In such cases it is considered following the associated propagation loss.

2.1 Attenuation due to atmospheric gases

Some attenuation due to absorption by oxygen and water vapour is always present, and should be included in the calculation of total propagation loss at frequencies above about 10 GHz. The attenuation on a path of length d (km) is given by:

$$A_a = \gamma_a \, d \qquad \text{dB} \tag{1}$$

The specific attenuation γ_a (dB/km) should be obtained using Recommendation ITU-R P.676.

NOTE 1 – On long paths at frequencies above about 20 GHz, it may be desirable to take into account known statistics of water vapour density and temperature in the vicinity of the path. Information on water vapour density is given in Recommendation ITU-R P.836.

2.2 Diffraction fading

Variations in atmospheric refractive conditions cause changes in the effective Earth's radius or k-factor from its median value of approximately 4/3 for a standard atmosphere (see Recommendation ITU-R P.310). When the atmosphere is sufficiently sub-refractive (large positive values of the gradient of refractive index, low k-factor values), the ray paths will be bent in such a way that the Earth appears to obstruct the direct path between transmitter and receiver, giving rise to the kind of fading called diffraction fading. This fading is the factor that determines the antenna heights.

k-factor statistics for a single point can be determined from measurements or predictions of the refractive index gradient in the first 100 m of the atmosphere (see Recommendation ITU-R P.453 on effects of refraction). These gradients need to be averaged in order to obtain the effective value of k for the path length in question, k_e. Values of k_e exceeded for 99.9% of the time are discussed in terms of path clearance criteria in the following section.

2.2.1 Diffraction loss dependence on path clearance

Diffraction loss will depend on the type of terrain and the vegetation. For a given path ray clearance, the diffraction loss will vary from a minimum value for a single knife-edge obstruction to a maximum for smooth spherical Earth. Methods for calculating diffraction loss for these two cases and also for paths with irregular terrain are discussed in Recommendation ITU-R P.526. These upper and lower limits for the diffraction loss are shown in Fig. 1.

FIGURE 1

Diffraction loss for obstructed line-of-sight microwave radio paths

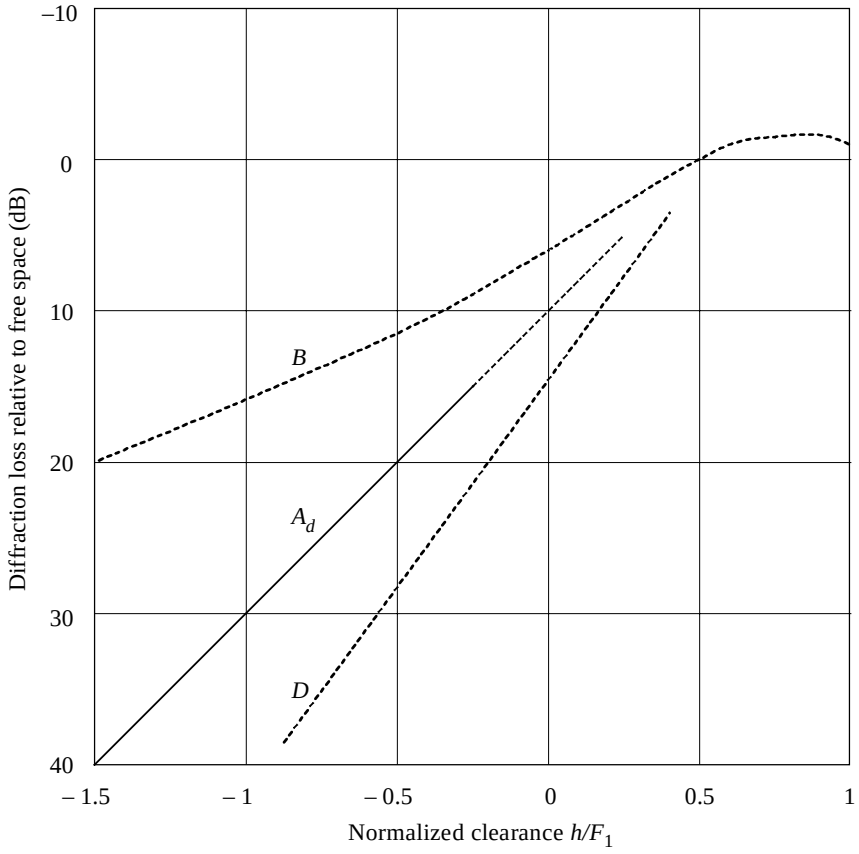

B: theoretical knife-edge loss curve
D: theoretical smooth spherical Earth loss curve, at 6.5 GHz and k_e = 4/3
A_d: empirical diffraction loss based on equation (2) for intermediate terrain
h: amount by which the radio path clears the Earth's surface
F_1: radius of the first Fresnel zone

0530-01

The diffraction loss over average terrain can be approximated for losses greater than about 15 dB by the formula:

$$A_d = -20\, h/F_1 + 10 \quad \text{dB} \tag{2}$$

where h is the height difference (m) between most significant path blockage and the path trajectory (h is negative if the top of the obstruction of interest is above the virtual line-of-sight) and F_1 is the radius of the first Fresnel ellipsoid given by:

$$F_1 = 17.3 \sqrt{\frac{d_1 \; d_2}{f \; d}} \quad \text{m} \tag{3}$$

with:

f: frequency (GHz)

d: path length (km)

d_1 and d_2: distances (km) from the terminals to the path obstruction.

A curve, referred to as A_d, based on equation (2) is also shown in Fig. 1. This curve, strictly valid for losses larger than 15 dB, has been extrapolated up to 6 dB loss to fulfil the need of link designers.

2.2.2 Planning criteria for path clearance

At frequencies above about 2 GHz, diffraction fading of this type has in the past been alleviated by installing antennas that are sufficiently high, so that the most severe ray bending would not place the receiver in the diffraction region when the effective Earth radius is reduced below its normal value. Diffraction theory indicates that the direct path between the transmitter and the receiver needs a clearance above ground of at least 60% of the radius of the first Fresnel zone to achieve free-space propagation conditions. Recently, with more information on this mechanism and the statistics of k_e that are required to make statistical predictions, some administrations are installing antennas at heights that will produce some small known outage.

In the absence of a general procedure that would allow a predictable amount of diffraction loss for various small percentages of time and therefore a statistical path clearance criterion, the following procedure is advised for temperate and tropical climates.

2.2.2.1 Non-diversity antenna configurations

Step 1: Determine the antenna heights required for the appropriate median value of the point k-factor (see § 2.2; in the absence of any data, use $k = 4/3$) and 1.0 F_1 clearance over the highest obstacle (temperate and tropical climates);

Step 2: Obtain the value of k_e (99.9%) from Fig. 2 for the path length in question;

Step 3: Calculate the antenna heights required for the value of k_e obtained from Step 2 and the following Fresnel zone clearance radii:

Temperate climate	Tropical climate
0.0 F_1 (i.e. grazing) if there is a single isolated path obstruction 0.3 F_1 if the path obstruction is extended along a portion of the path	0.6 F_1 for path lengths greater than about 30 km

Step 4: Use the larger of the antenna heights obtained by Steps 1 and 3.

In cases of uncertainty as to the type of climate, the more conservative clearance rule for tropical climates may be followed or at least a rule based on an average of the clearances for temperate and tropical climates. Smaller fractions of F_1 may be necessary in Steps 1 and 3 above for frequencies less than about 2 GHz in order to avoid unacceptably large antenna heights.

Higher fractions of F_1 may be necessary in Step 3 for frequencies greater than about 10 GHz in order to reduce the risk of diffraction in sub-refractive conditions.

FIGURE 2

Value of k_e exceeded for approximately 99.9% of the worst month (Continental temperate climate)

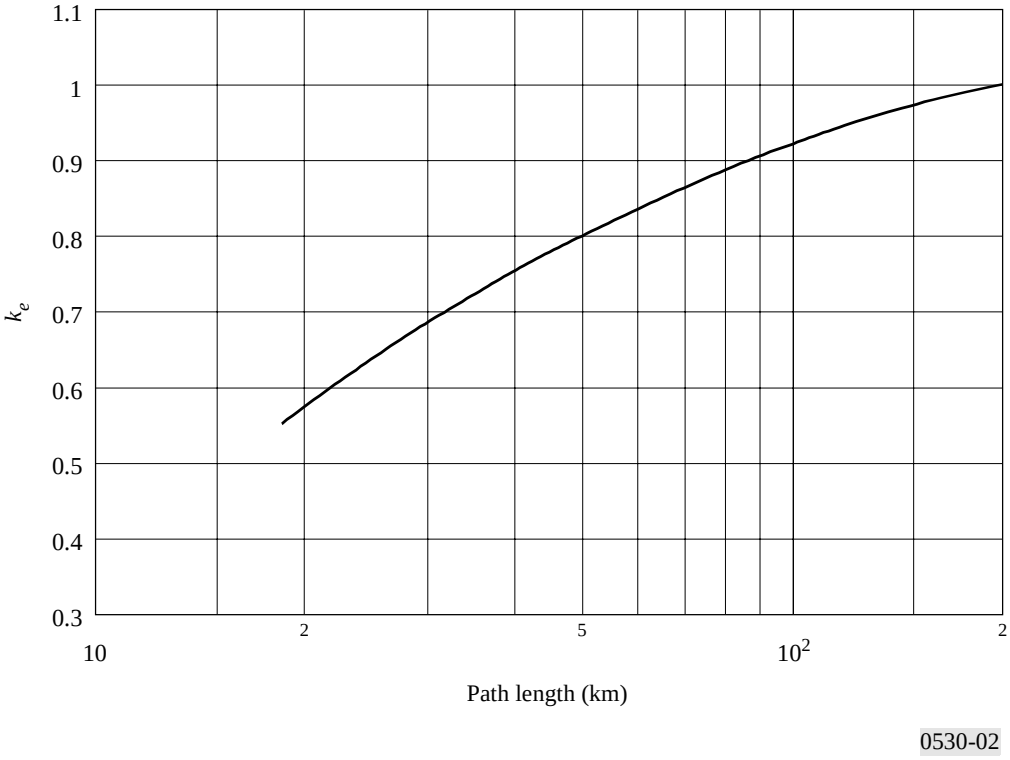

2.2.2.2 Two antenna space-diversity configurations

Step 1: Calculate the height of the lower antenna for the appropriate median value of the point *k*-factor (in the absence of any data use $k = 4/3$) and the following Fresnel zone clearances:

0.6 F_1 to 0.3 F_1 if the path obstruction is extended along a portion of the path;

0.3 F_1 to 0.0 F_1 if there are one or two isolated obstacles on the path profile.

One of the lower values in the two ranges noted above may be chosen if necessary to avoid increasing heights of existing towers or if the frequency is less than 2 GHz.

Alternatively, the clearance of the lower antenna may be chosen to give about 6 dB of diffraction loss during normal refractivity conditions (i.e. during the middle of the day), or some other loss appropriate to the fade margin of the system, as determined by test measurements. Measurements should be carried out on several different days to avoid anomalous refractivity conditions.

In this alternative case the diffraction loss can also be estimated using Fig. 1 or equation (2).

Step 2: Calculate the height of the upper antenna using the procedure for single antenna configurations noted above.

Step 3: Verify that the spacing of the two antennas satisfies the requirements for diversity under multipath fading conditions. If not, increase the height of the upper antenna accordingly.

This fading, which results when the path is obstructed or partially obstructed by the terrain during sub-refractive conditions, is the factor that governs antenna heights.

2.3 Fading and enhancement due to multipath and related mechanisms

Various clear-air fading mechanisms caused by extremely refractive layers in the atmosphere must be taken into account in the planning of links of more than a few kilometres in length; beam spreading (commonly referred to as defocusing), antenna decoupling, surface multipath, and atmospheric multipath. Most of these mechanisms can occur by themselves

or in combination with each other (see Note 1). A particularly severe form of frequency selective fading occurs when beam spreading of the direct signal combines with a surface reflected signal to produce multipath fading. Scintillation fading due to smaller scale turbulent irregularities in the atmosphere is always present with these mechanisms but at frequencies below about 40 GHz its effect on the overall fading distribution is not significant.

NOTE 1 – Antenna decoupling governs the minimum beamwidth of the antennas that should be chosen.

A method for predicting the single-frequency (or narrow-band) fading distribution at large fade depths in the average worst month in any part of the world is given in § 2.3.1. This method does not make use of the path profile and can be used for initial planning, licensing, or design purposes. A second method in § 2.3.2 that is suitable for all fade depths employs the method for large fade depths and an interpolation procedure for small fade depths.

A method for predicting signal enhancement is given in § 2.3.3. The method uses the fade depth predicted by the method in § 2.3.1 as the only input parameter. Finally, a method for converting average worst month to average annual distributions is given in § 2.3.4.

2.3.1 Method for small percentages of time

This method is described as a step-by-step procedure in § 2.3.1.1 to 2.3.1.3.

2.3.1.1 For the path location in question, estimate the geoclimatic factor, K, for the average worst month from fading data for the geographic area of interest if these are available (see Appendix 1).

Inland links: If measured data for K are not available, K can be estimated for links in inland areas (see Note 1 for definition of inland links) from the following empirical relation in the climatic variable p_L (i.e., the percentage of time that the refractivity gradient in the lowest 100 m of the atmosphere is more negative than –100 N units/km in the estimated average worst month; see below):

$$K = 5.0 \times 10^{-7} \times 10^{-0.1(C_0 - C_{Lat} - C_{Lon})} p_L^{1.5} \quad (4)$$

The value of the coefficient C_0 in equation (4) is given in Table 1 for three ranges of altitude of the lower of the transmitting and receiving antennas and three types of terrain (plains, hills, or mountains). In cases of uncertainty as to whether a link should be classified as being in a plains or hilly area, the mean value of the coefficients C_0 for these two types of area should be employed. Similarly, in cases of uncertainty as to whether a link should be classified as being in a hilly or mountainous area, the mean value of the coefficients C_0 for these two types of area should be employed. Links traversing plains at one end and mountains at the other should be classified as being in hilly areas. For the purposes of deciding whether a partially overwater path is in a largely plains, hilly, or mountainous area, the water surface should be considered as a plain.

For planning purposes where the type of terrain is not known, the following values of the coefficient C_0 in equation (4) should be employed:

$C_0 = 1.7$ for lower-altitude antenna in the range 0-400 m above mean sea level;

$C_0 = 4.2$ for lower-altitude antenna in the range 400-700 m above mean sea level;

$C_0 = 8$ for lower-altitude antenna more than 700 m above mean sea level.

The coefficient C_{Lat} in equation (4) of latitude ξ is given by:

$$C_{Lat} = 0 \quad \text{dB} \quad \text{for } \xi \leq 53° \text{ N or °S} \quad (5)$$

$$C_{Lat} = -53 + \xi \quad \text{dB} \quad \text{for } 53° \text{ N or °S} < \xi < 60° \text{ N or °S} \quad (6)$$

$$C_{Lat} = 7 \quad \text{dB} \quad \text{for } \xi \geq 60° \text{ N or °S} \quad (7)$$

and the longitude coefficient C_{Lon}, by:

$$C_{Lon} = 3 \quad \text{dB} \quad \text{for longitudes of Europe and Africa} \quad (8)$$

$$C_{Lon} = -3 \quad \text{dB} \quad \text{for longitudes of North and South America} \quad (9)$$

$$C_{Lon} = 0 \quad \text{dB} \quad \text{for all other longitudes} \quad (10)$$

TABLE 1

Values of coefficient C_0 in equations (4) and (13) for three ranges of lower antenna altitude and three types of terrain

Altitude of lower antenna and type of link terrain	C_0 (dB)
Low altitude antenna (0-400 m) – Plains: Overland or partially overland links, with lower-antenna altitude less than 400 m above mean sea level, located in largely plains areas	0
Low altitude antenna (0-400 m) – Hills: Overland or partially overland links, with lower-antenna altitude less than 400 m above mean sea level, located in largely hilly areas	3.5
Medium altitude antenna (400-700 m) – Plains: Overland or partially overland links, with lower-antenna altitude in the range 400-700 m above mean sea level, located in largely plains areas	2.5
Medium altitude antenna (400-700 m) – Hills: Overland or partially overland links, with lower-antenna altitude in the range 400-700 m above mean sea level, located in largely hilly areas	6
High altitude antenna (>700 m) – Plains: Overland or partially overland links, with lower-antenna altitude more than 700 m above mean sea level, located in largely plains areas	5.5
High altitude antenna (>700 m) – Hills: Overland or partially overland links, with lower-antenna altitude more than 700 m above mean sea level, located in largely hilly areas	8
High altitude antenna (>700 m) – Mountains: Overland or partially overland links, with lower-antenna altitude more than 700 m above mean sea level, located in largely mountainous areas	10.5

The value of the climatic variable p_L in equation (4) is estimated by taking the highest value of the –100 N units/km gradient exceedance from the maps for the four seasonally representative months of February, May, August and November given in Figs. 7 to 10 of Recommendation ITU-R P.453. An exception to this is that only the maps for May and August should be used for latitudes greater than 60° N or 60° S.

It may be desirable in some cases to obtain expansions of the maps in Figs. 7 to 10 of Recommendation ITU-R P.453 in the area of the link in question and accurately plot the point corresponding to the centre of the link to obtain the p_L value. Since the maps are on a Mercator projection, the following relation should be employed to accurately plot the centre point latitude ξ:

$$\Delta z_L = \Delta z \left[\frac{\ln\left[\tan\left(45^\circ + 0.5\,\xi\right)\right] - \ln\left[\tan\left(45^\circ + 0.5\,\xi_1\right)\right]}{\ln\left[\tan\left(45^\circ + 0.5\,\xi_2\right)\right] - \ln\left[\tan\left(45^\circ + 0.5\,\xi_1\right)\right]} \right] \tag{11}$$

Here Δz is the distance (e.g. in mm) between the nearest lower and upper latitude grid lines at latitudes ξ_1 and ξ_2, respectively (e.g. 30° and 45°); Δz_L is the required distance (e.g. in mm) between the lower latitude grid line and the point corresponding to the centre of the link. The centre point longitude can be plotted by linear interpolation.

Coastal links over/near large bodies of water: if measured data for K are not available for coastal links (see Note 2 for definition) over/near large bodies of water (see Note 3 for definition of large bodies of water), K can be estimated from:

$$K = \begin{cases} K_l(r_c) = 10^{(1 - r_c)\log K_i + r_c \log K_{cl}} & \text{for } K_{cl} \geq K_i \\ K_i & \text{for } K_{cl} < K_i \end{cases} \tag{12}$$

where r_c is the fraction of the path profile below 100 m altitude above the mean level of the body of water in question and within 50 km of the coastline, but without an intervening height of land above 100 m altitude, K_i is given by the expression for K in equation (4), and:

$$K_{cl} = 2.3 \times 10^{-4} \times 10^{-0.1C_0 - 0.011|\xi|} \tag{13}$$

with C_0 given in Table 1. Note that the condition $K_{cl} < K_i$ in equation (12) occurs in a few regions at low and mid latitudes.

Coastal links over/near medium-sized bodies of water: if measured data for K are not available for coastal links (see Note 2 for definition) over/near medium-sized bodies of water (see Note 3 for definition of medium-sized bodies of water), K can be estimated from:

$$K = \begin{cases} K_m(r_c) = 10^{(1 - r_c)\log K_i + r_c \log K_{cm}} & \text{for } K_{cm} \geq K_i \\ K_i & \text{for } K_{cm} < K_i \end{cases} \tag{14}$$

and

$$K_{cm} = 10^{0.5(\log K_i + \log K_{cl})} \tag{15}$$

with K_{cl} given by equation (13). Note that the condition $K_{cm} < K_i$ in equation (15) occurs in a few regions at low and mid latitudes.

NOTE 1 – Inland links are those in which either the entire path profile is above 100 m altitude (with respect to mean sea level) or beyond 50 km from the nearest coastline, or in which part or all of the path profile is below 100 m altitude for a link entirely within 50 km of the coastline, but there is an intervening height of land higher than 100 m between this part of the link and the coastline. Links passing over a river or a small lake should normally be classed as passing over land. For links in a region of many lakes, see Note 4.

NOTE 2 – The link may be considered to be crossing a coastal area if a fraction r_c of the path profile is less than 100 m above the mean level of a medium-sized or large body of water and within 50 km of its coastline, and if there is no height of land above the 100 m altitude (relative to the mean altitude of the body of water in question) between this fraction of the path profile and the coastline.

NOTE 3 – The size of a body of water can be chosen on the basis of several known examples: Medium-sized bodies of water include the Bay of Fundy (east coast of Canada) and the Strait of Georgia (west coast of Canada), the Gulf of Finland, and other bodies of water of similar size. Large bodies of water include the English Channel, the North Sea, the larger reaches of the Baltic and Mediterranean Seas, Hudson Strait, and other bodies of water of similar size or larger. In cases of uncertainty as to whether the size of body of water in question should be classed as medium or large, K should be calculated from:

$$K = 10^{(1 - r_c)\log K_i + 0.5\, r_c (\log K_{cm} + \log K_{cl})} \tag{16}$$

NOTE 4 – Regions (not otherwise in coastal areas) in which there are many lakes over a fairly large area are believed to behave somewhat like coastal areas. The region of lakes in southern Finland provides the best known example. Until such regions can be better defined, K should be calculated from:

$$K = 10^{0.5[(2 - r_c)\log K_i + r_c \log K_{cm}]} \tag{17}$$

2.3.1.2 From the antenna heights h_e and h_r (in metres above sea level or some other reference height), calculate the magnitude of the path inclination $|\varepsilon_p|$ (mrad) from:

$$\left|\varepsilon_p\right| = \left|h_r - h_e\right| / d \tag{18}$$

where d, is the path length (km).

2.3.1.3 Calculate the percentage of time p_w that fade depth A (dB) is exceeded in the average worst month from:

$$p_w = K\, d^{3.6}\, f^{0.89} \left(1 + \left|\varepsilon_p\right|\right)^{-1.4} \times 10^{-A/10} \quad \% \tag{19}$$

where f is the frequency (GHz).

Equation (19) applies only to narrow-band systems. It is considered valid for fade depths greater than about 15 dB or the value exceeded for 0.1% of the worst month, whichever is greater. However, for fade depths approaching these limits, the method of § 2.3.2 should be applied to avoid potential errors.

For prediction of exceedance percentages for the average year instead of the average worst month, see § 2.3.4.

NOTE 1 – Equation (19) was derived from fading data on paths with lengths in the range 7-95 km, frequencies in the range 2-37 GHz and path inclinations for the range 0-24 mrad. Checks using several other sets of data for paths up to 237 km in length and frequencies as low as 500 MHz suggest, however, that it is valid for larger ranges of path length and frequency. The results of a semi-empirical analysis indicate that the lower frequency limit of validity is inversely proportional to path length. A rough estimate of this lower frequency limit, f_{min}, can be obtained from:

$$f_{min} = 15 / d \qquad \text{GHz} \tag{20}$$

2.3.2 Method for various percentages of time

The method given below for predicting the percentage of time that any fade depth is exceeded combines the deep fading distribution given in the preceding section and an empirical interpolation procedure for shallow fading down to 0 dB.

Step 1: Using the method in § 2.3.1 calculate the multipath occurrence factor, p_0 (i.e., the intercept of the deep-fading distribution with the percentage of time-axis):

$$p_0 = K\, d^{3.6}\, f^{0.89} \left(1 + \left|\varepsilon_p\right|\right)^{-1.4} \tag{21}$$

Note that equation (21) is equivalent to equation (19) with $A = 0$.

The value of p_0 represents the effects of radio-climatic factor, K, the path length and inclination, and the frequency. The method is valid for values of p_0 up to 2 000.

Step 2: Calculate the value of fade depth, A_t, at which the transition occurs between the deep-fading distribution and the shallow-fading distribution as predicted by the empirical interpolation procedure:

$$A_t = 25 + 1.2 \log p_0 \qquad \text{dB} \tag{22}$$

The procedure now depends on whether A is greater or less than A_t.

Step 3a: If the required fade depth, A, is equal to or greater than A_t:

Calculate the percentage of time that A is exceeded in the average worst month:

$$p_w = p_0 \times 10^{-A/10} \qquad \% \tag{23}$$

Note that equation (23) is equivalent to equation (19).

Step 3b: If the required fade depth, A, is less than A_t:

Calculate the percentage of time, p_t, that A_t is exceeded in the average worst month:

$$p_t = p_0 \times 10^{-A_t/10} \qquad \% \tag{24}$$

Note that equation (24) is equivalent to equation (19) with $A = A_t$.

Calculate q'_a from the transition fade A_t and transition percentage time p_t:

$$q'_a = -20 \log_{10} \left\{ -\ln \left[\left(100 - p_t \right) / 100 \right] \right\} / A_t \tag{25}$$

Calculate q_t from q'_a and the transition fade A_t:

$$q_t = \left(q'_a - 2\right) \Big/ \left[\left(1 + 0.3 \times 10^{-A_t/20}\right) 10^{-0.016 A_t} \right] - 4.3 \left(10^{-A_t/20} + A_t/800\right) \tag{26}$$

Calculate q_a from the required fade A:

$$q_a = 2 + \left[1 + 0.3 \times 10^{-A/20}\right]\left[10^{-0.016\,A}\right]\left[q_t + 4.3\left(10^{-A/20} + A/800\right)\right] \quad (27)$$

Calculate the percentage of time, p_w, that the fade depth A (dB) is exceeded in the average worst month:

$$p_w = 100\left[1 - \exp\left(-10^{-q_a\,A/20}\right)\right] \quad \% \quad (28)$$

Provided that $p_0 < 2\,000$, the above procedure produces a monotonic variation of p_w versus A which can be used to find A for a given value of p_w using simple iteration.

With p_0 as a parameter, Fig. 3 gives a family of curves providing a graphical representation of the method.

FIGURE 3

Percentage of time, p_w, fade depth, A, exceeded in an average worst month, with p_0 (in equation (21)) ranging from 0.01 to 1 000

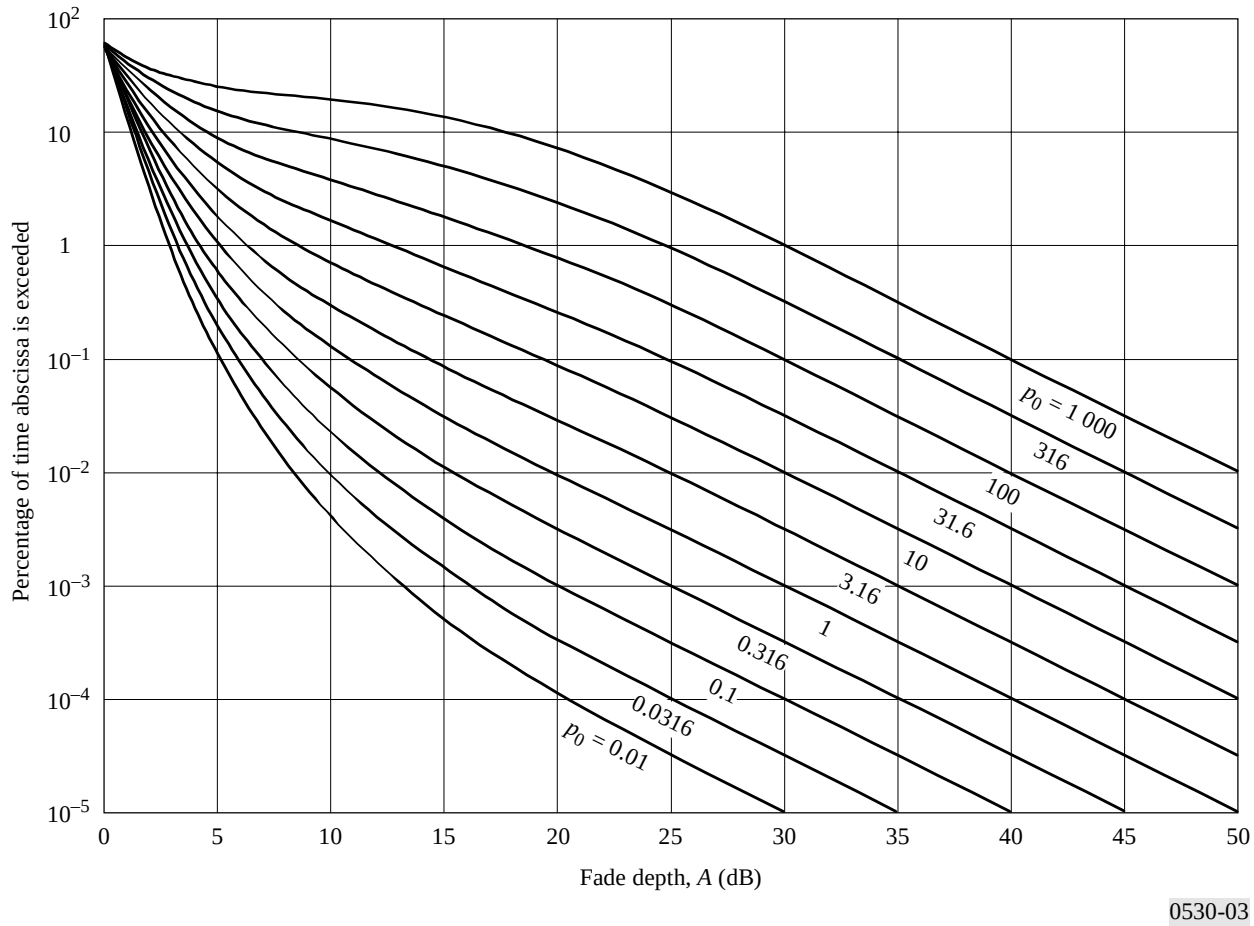

2.3.3 Prediction method for enhancement

Large enhancements are observed during the same general conditions of frequent ducts that result in multipath fading. Average worst month enhancement above 10 dB should be predicted using:

$$p_w = 100 - 10^{(-1.7 + 0.2\,A_{0.01} - E)/3.5} \quad \% \quad \text{for } E > 10\,\text{dB} \quad (29)$$

where E (dB) is the enhancement not exceeded for p% of the time and $A_{0.01}$ is the predicted deep fade depth using equation (19) exceeded for $p_w = 0.01$% of the time.

For the enhancement between 10 and 0 dB use the following step-by-step procedure:

Step 1: Calculate the percentage of time p'_w with enhancement less or equal to 10 dB ($E' = 10$) using equation (29).

Step 2: Calculate q'_e using:

$$q'_e = -\frac{20}{E'}\left(\log_{10}\left[-\ln\left(1-\frac{100 - p'_w}{58.21}\right)\right]\right) \quad (30)$$

Step 3: Calculate the parameter q_s from:

$$q_s = 2.05\ q'_e - 20.3 \quad (31)$$

Step 4: Calculate q_e for the desired E using:

$$q_e = 8 + \left[1 + 0.3 \times 10^{-E/20}\right]\left[10^{-0.7E/20}\right]\left[q_s + 12\left(10^{-E/20} + E/800\right)\right] \quad (32)$$

Step 5: The percentage of time that the enhancement E (dB) is not exceeded is found from:

$$p_w = 100 - 58.21\left[1 - \exp\left(-10^{-q_e E/20}\right)\right] \quad (33)$$

The set of curves in Fig. 4 gives a graphical representation of the method with p_0 as parameter; (see equation (21)). Each curve in Fig. 4 corresponds to the curve in Fig. 3 with the same value of p_0. It should be noted that Fig. 4 gives the percentage of time for which the enhancements are exceeded which corresponds to $(100 - p_w)$, with p_w given by equations (29) and (33).

FIGURE 4

Percentage of time, $(100 - p_w)$, enhancement, E, exceeded in the average worst month, with p_0 (in equation (21)) ranging from 0.01 to 1 000

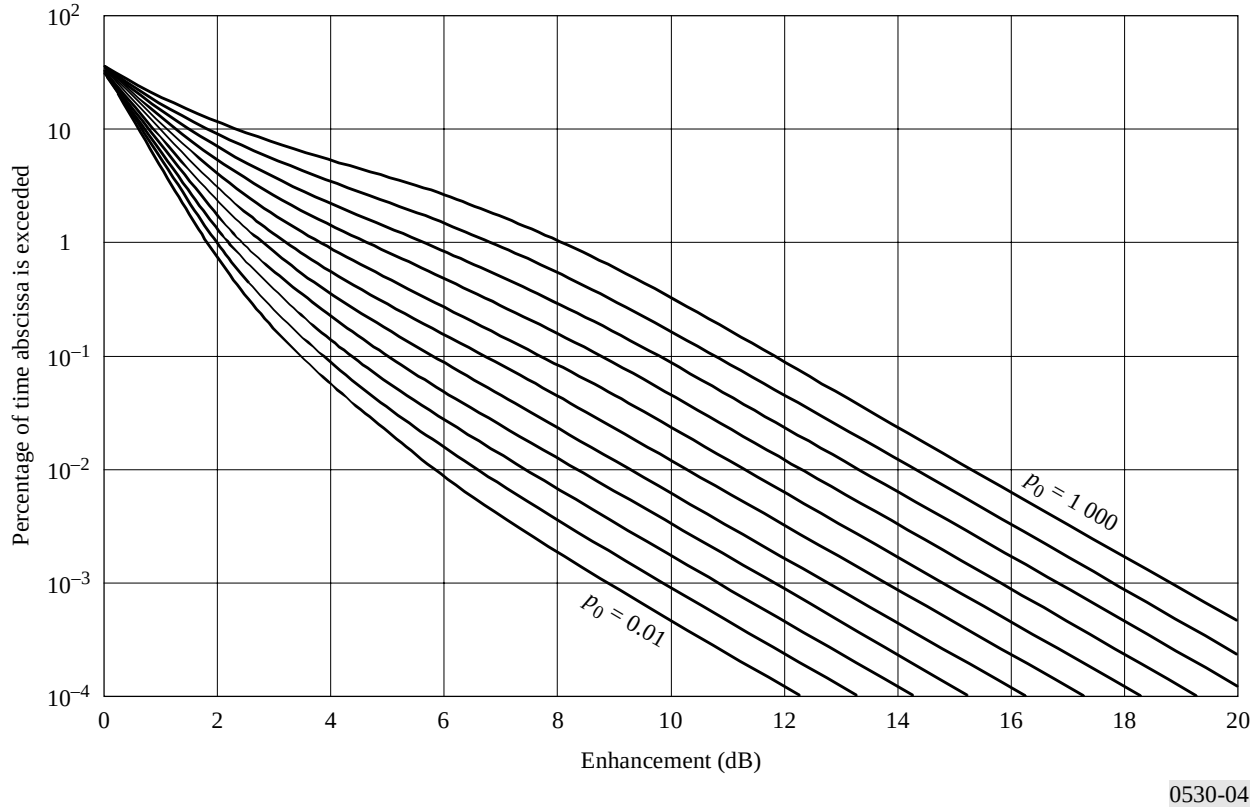

For prediction of exceedance percentages for the average year instead of the average worst month, see § 2.3.4.

2.3.4 Conversion from average worst month to average annual distributions

The fading and enhancement distributions for the average worst month obtained from the methods of § 2.3.1 to 2.3.3 can be converted to distributions for the average year by employing the following procedure:

Step 1: Calculate the percentage of time p_w fade depth A is exceeded in the large tail of the distribution for the average worst month from equation (19).

Step 2: Calculate the logarithmic geoclimatic conversion factor ΔG from:

$$\Delta G = 10.5 - 5.6 \log\left(1.1 \pm |\cos 2\xi|^{0.7}\right) - 2.7 \log d + 1.7 \log\left(1 + |\varepsilon_p|\right) \quad \text{dB} \tag{34}$$

where $\Delta G \leq 10.8$ dB and the positive sign in equation (34) is employed for $\xi \leq 45°$ and the negative sign for $\xi > 45°$, and where:

ξ: latitude (°N or °S)

d: path length (km)

$|\varepsilon_p|$: magnitude of path inclination (obtained from equation (18)).

Step 3: Calculate the percentage of time p fade depth A is exceeded in the large fade depth tail of the distribution for the average year from:

$$p = 10^{-\Delta G/10} p_w \quad \% \tag{35}$$

Step 4: If the shallow fading range of the distribution is required (i.e. $A < 25$ dB or $A < 35$ dB, as appropriate) follow the method of § 2.3.2, replacing p_w by p.

Step 5: If it is required to predict the distribution of enhancement for the average year, follow the method of § 2.3.3, where $A_{0.01}$ is now the fade depth exceeded for 0.01% of the time in the average year. Obtain first p_w by inverting equation (35) and using $p = 0.01\%$. Then obtain fade depth $A_{0.01}$ exceeded for 0.01% of the time in the average year by inverting equation (19) and using p in place of p_w.

2.3.5 Prediction of non-selective outage (see Note 1)

In the design of a digital link, calculate the probability of outage P_{ns} due to the non-selective component of the fading (see § 7) from:

$$P_{ns} = p_w / 100 \tag{36}$$

where p_w(%) is the percentage of time that the flat fade margin $A = F$ (dB) corresponding to the specified bit error ratio (BER) is exceeded in the average worst month (obtained from § 2.3.1 or § 2.3.2, as appropriate). The flat fade margin, F, is obtained from the link calculation and the information supplied with the particular equipment, also taking into account possible reductions due to interference in the actual link design.

NOTE 1 – The outage is defined as the probability that the BER is larger than a given threshold (see § 7 for further information).

2.3.6 Occurrence of simultaneous fading on multi-hop links

Experimental evidence indicates that, in clear-air conditions, fading events exceeding 20 dB on adjacent hops in a multi-hop link are almost completely uncorrelated. This suggests that, for analogue systems with large fade margins, the outage time for a series of hops in tandem is approximately given by the sum of the outage times for the individual hops.

For fade depths not exceeding 10 dB, the probability of simultaneously exceeding a given fade depth on two adjacent hops can be estimated from:

$$P_{12} = (P_1 \ P_2)^{0.8} \tag{37}$$

where P_1 and P_2 are the probabilities of exceeding this fade depth on each individual hop (see Note 1).

The correlation between fading on adjacent hops decreases with increasing fade depth between 10 and 20 dB, so that the probability of simultaneously exceeding a fade depth greater than 20 dB can be approximately expressed by:

$$P_{12} = P_1 \; P_2 \tag{38}$$

NOTE 1 – The correlation between fading on adjacent hops is expected to be dependent on path length. Equation (37) is an average based on the results of measurements on 47 pairs of adjacent line-of-sight hops operating in the 5 GHz band, with path lengths in the range 11-97 km, and an average path length of approximately 45 km.

2.4 Attenuation due to hydrometeors

Attenuation can also occur as a result of absorption and scattering by such hydrometeors as rain, snow, hail and fog. Although rain attenuation can be ignored at frequencies below about 5 GHz, it must be included in design calculations at higher frequencies, where its importance increases rapidly. A technique for estimating long-term statistics of rain attenuation is given in § 2.4.1. On paths at high latitudes or high altitude paths at lower latitudes, wet snow can cause significant attenuation over an even larger range of frequencies. More detailed information on attenuation due to hydrometeors other than rain is given in Recommendation ITU-R P.840.

At frequencies where both rain attenuation and multipath fading must be taken into account, the exceedance percentages for a given fade depth corresponding to each of these mechanisms can be added.

2.4.1 Long-term statistics of rain attenuation

The following simple technique may be used for estimating the long-term statistics of rain attenuation:

Step 1: Obtain the rain rate $R_{0.01}$ exceeded for 0.01% of the time (with an integration time of 1 min). If this information is not available from local sources of long-term measurements, an estimate can be obtained from the information given in Recommendation ITU-R P.837.

Step 2: Compute the specific attenuation, γ_R (dB/km) for the frequency, polarization and rain rate of interest using Recommendation ITU-R P.838.

Step 3: Compute the effective path length d_{eff} of the link by multiplying the actual path length d by a distance factor r. An estimate of this factor is given by:

$$r = \frac{1}{1 + d / d_0} \tag{39}$$

where, for $R_{0.01} \leq 100$ mm/h:

$$d_0 = 35 \, e^{-0.015 \, R_{0.01}} \tag{40}$$

For $R_{0.01} > 100$ mm/h, use the value 100 mm/h in place of $R_{0.01}$.

Step 4: An estimate of the path attenuation exceeded for 0.01% of the time is given by:

$$A_{0.01} = \gamma_R \, d_{eff} = \gamma_R \, dr \qquad \text{dB} \tag{41}$$

Step 5: For radio links located in latitudes equal to or greater than 30° (North or South), the attenuation exceeded for other percentages of time p in the range 0.001% to 1% may be deduced from the following power law:

$$\frac{A_p}{A_{0.01}} = 0.12 \; p^{-(0.546 \; + \; 0.043 \; \log_{10} p)} \tag{42}$$

This formula has been determined to give factors of 0.12, 0.39, 1 and 2.14 for 1%, 0.1%, 0.01% and 0.001% respectively, and must be used only within this range.

Step 6: For radio links located at latitudes below 30° (North or South), the attenuation exceeded for other percentages of time p in the range 0.001% to 1% may be deduced from the following power law:

$$\frac{A_p}{A_{0.01}} = 0.07\ p^{-(0.855\ +\ 0.139 \log_{10} p)} \tag{43}$$

This formula has been determined to give factors of 0.07, 0.36, 1 and 1.44 for 1%, 0.1%, 0.01% and 0.001%, respectively, and must be used only within this range.

Step 7: If worst-month statistics are desired, calculate the annual time percentages p corresponding to the worst-month time percentages p_w using climate information specified in Recommendation ITU-R P.841. The values of A exceeded for percentages of the time p on an annual basis will be exceeded for the corresponding percentages of time p_w on a worst-month basis.

The prediction procedure outlined above is considered to be valid in all parts of the world at least for frequencies up to 40 GHz and path lengths up to 60 km.

2.4.2 Frequency scaling of long-term statistics of rain attenuation

When reliable long-term attenuation statistics are available at one frequency the following empirical expression may be used to obtain a rough estimate of the attenuation statistics for other frequencies in the range 7 to 50 GHz, for the same hop length and in the same climatic region:

$$A_2 = A_1\ (\Phi_2\ /\ \Phi_1)^{1\ -\ H(\Phi_1,\ \Phi_2,\ A_1)} \tag{44}$$

where:

$$\Phi(f) = \frac{f^2}{1 + 10^{-4}\ f^2} \tag{45}$$

$$H(\Phi_1, \Phi_2, A_1) = 1.12 \times 10^{-3} (\Phi_2 / \Phi_1)^{0.5} (\Phi_1\ A_1)^{0.55} \tag{46}$$

Here, A_1 and A_2 are the equiprobable values of the excess rain attenuation at frequencies f_1 and f_2 (GHz), respectively.

2.4.3 Polarization scaling of long-term statistics of rain attenuation

Where long-term attenuation statistics exist at one polarization (either vertical (V) or horizontal (H)) on a given link, the attenuation for the other polarization over the same link may be estimated through the following simple formulae:

$$A_V = \frac{300\ A_H}{335\ +\ A_H} \quad \text{dB} \tag{47}$$

or

$$A_H = \frac{335\ A_V}{300\ -\ A_V} \quad \text{dB} \tag{48}$$

These expressions are considered to be valid in the range of path length and frequency for the prediction method of § 2.4.1.

2.4.4 Statistics of event duration and number of events

Although there is little information as yet on the overall distribution of fade duration, there are some data and an empirical model for specific statistics such as mean duration of a fade event and the number of such events. An observed difference between the average and median values of duration indicates, however, a skewness of the overall distribution of duration. Also, there is strong evidence that the duration of fading events in rain conditions is much longer than those during multipath conditions.

An attenuation event is here defined to be the exceedance of attenuation A for a certain period of time (e.g., 10 s or longer). The relationship between the number of attenuation events $N(A)$, the mean duration $D_m(A)$ of such events, and the total time $T(A)$ for which attenuation A is exceeded longer than a certain duration, is given by:

$$N(A) = T(A) / D_m(A) \tag{49}$$

The total time $T(A)$ depends on the definition of the event. The event usually of interest for application is one of attenuation A lasting for 10 s or longer. However, events of shorter duration (e.g., a sampling interval of 1 s used in an experiment) are also of interest for determining the percentage of the overall outage time attributed to unavailability (i.e., the total event time lasting 10 s or longer).

The number of fade events exceeding attenuation A for 10 s or longer can be represented by:

$$N_{10\,s}(A) = a\,A^b \tag{50}$$

where a and b are coefficients that are expected to depend on frequency, path length, and other variables such as climate.

On the basis of one set of measurements for an 18 GHz, 15 km path on the Scandinavian peninsula, values of a and b estimated for a one-year period are:

$$a = 5.7 \times 10^5 \qquad b = -3.4 \tag{51}$$

Once $N_{10\,s}(A)$ has been obtained from equation (50), the mean duration of fading events lasting 10 s or longer can be calculated by inverting equation (49).

Based on the noted set of measurements (from an 18 GHz, 15 km path on the Scandinavian peninsula), 95-100% of all rain events greater than about 15 dB can be attributed to unavailability. With such a fraction known, the availability can be obtained by multiplying this fraction by the total percentage of time that a given attenuation A is exceeded as obtained from the method of § 2.4.1.

2.4.5 Rain attenuation in multiple hop networks

There are several configurations of multiple hops of interest in point-to-point networks in which the non-uniform structure of hydrometeors plays a role. These include a series of hops in a tandem network and more than one such series of hops in a route-diversity network.

2.4.5.1 Length of individual hops in a tandem network

The overall transmission performance of a tandem network is largely influenced by the propagation characteristics of the individual hops. It is sometimes possible to achieve the same overall physical connection by different combinations of hop lengths. Increasing the length of individual hops inevitably results in an increase in the probability of outage for those hops. On the other hand, such a move could mean that fewer hops might be required and the overall performance of the tandem network might not be impaired.

2.4.5.2 Correlated fading on tandem hops

If the occurrence of rainfall were statistically independent of location, then the overall probability of fading for a linear series of links in tandem would be given to a good approximation by:

$$P_T = \sum_{i=1}^{n} P_i \tag{52}$$

where P_i is the ith of the total n links.

On the other hand, if precipitation events are correlated over a finite area, then the attenuation on two or more links of a multi-hop relay system will also be correlated, in which case the combined fading probability may be written as:

$$P_T = K \sum_{i=1}^{n} P_i \tag{53}$$

where K is a modification factor that includes the overall effect of rainfall correlation.

Few studies have been conducted with regard to this question. One such study examined the instantaneous correlation of rainfall at locations along an East-West route, roughly parallel to the prevailing direction of storm movement. Another monitored attenuation on a series of short hops oriented North-South, or roughly perpendicular to the prevailing storm track during the season of maximum rainfall.

For the case of links parallel to the direction of storm motion, the effects of correlation for a series of hops each more than 40 km in length, *l*, were slight. The modification factor, *K*, in this case exceeded 0.9 for rain induced outage of 0.03% and may reasonably be ignored (see Fig. 5). For shorter hops, however, the effects become more significant: the overall outage probability for 10 links of 20, 10 and 5 km each is approximately 80%, 65% and 40% of the uncorrelated expectation, respectively (modification factors 0.8, 0.65, 0.4). The influence of rainfall correlation is seen to be somewhat greater for the first few hops and then decreases as the overall length of the chain increases.

FIGURE 5

Modification factor for joint rain attenuation on a series of tandem hops of equal length, *l*, for an exceedance probability of 0.03% for each link

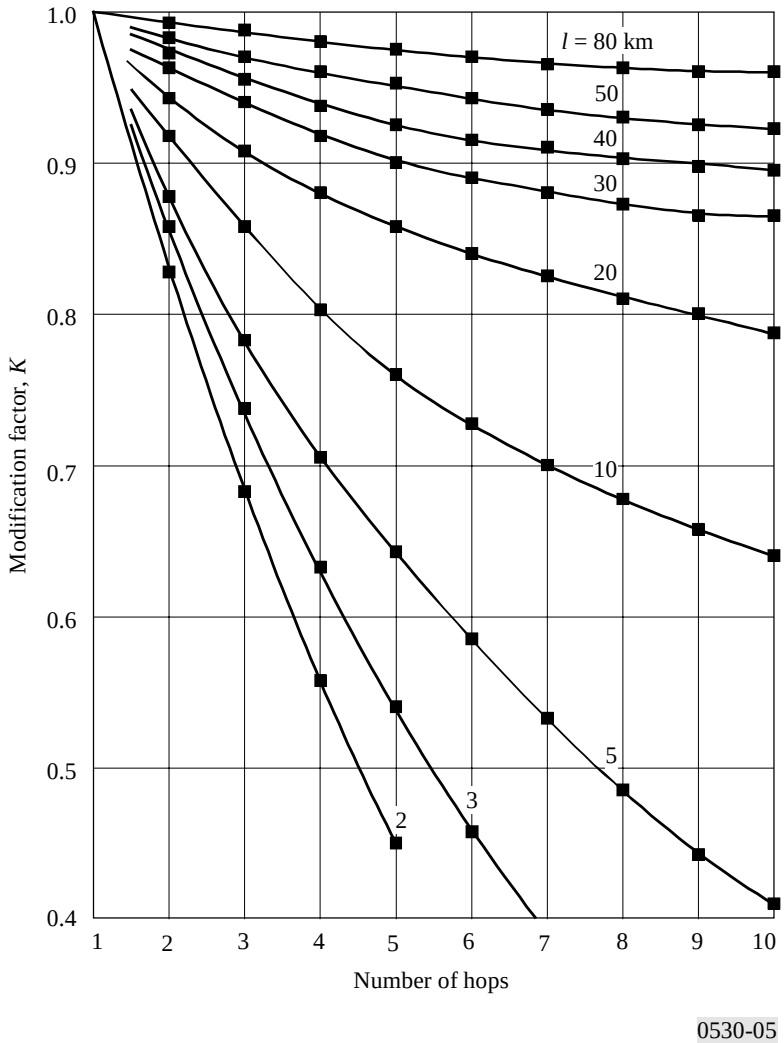

The modification factors for the case of propagation in a direction perpendicular to the prevailing direction of storm motion are shown in Fig. 6 for several probability levels. In this situation, the modification factors fall more rapidly for the first few hops (indicating a stronger short-range correlation than for propagation parallel to storm motion) and maintain relatively steady values thereafter (indicating a weaker long-range correlation).

FIGURE 6

Modification factor for joint rain attenuation on a series of tandem hops of approximately 4.6 km each for several exceedance probability levels for each link

(May 1975-March 1979)

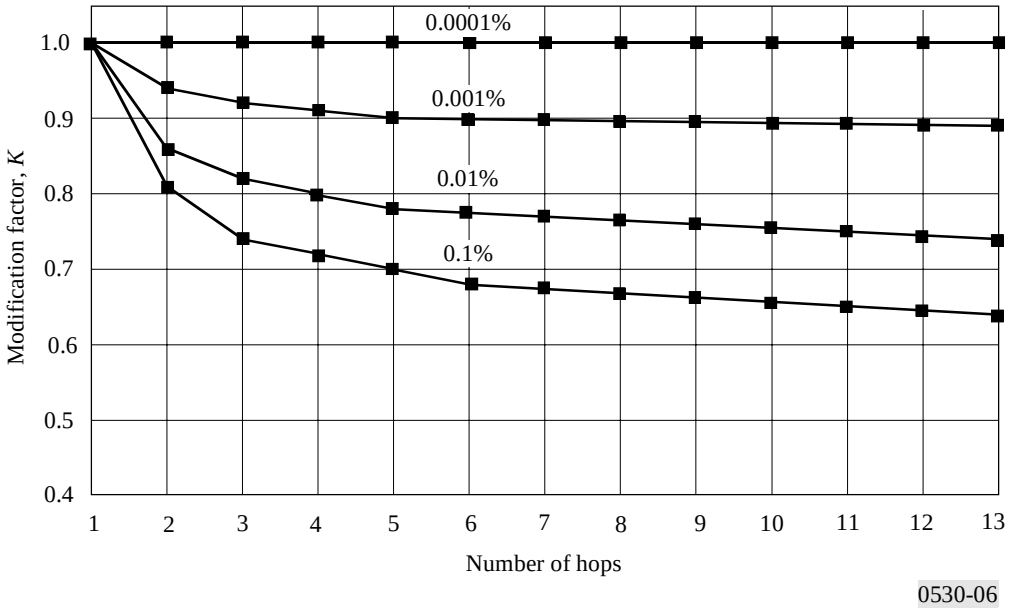

2.4.5.3 Route-diversity networks

Making use of the fact that the horizontal structure of precipitation can change significantly within the space of a fraction of a kilometre, route diversity networks can involve two or more hops in tandem in two or more diversity routes. Although there is no information on diversity improvement for complete route diversity networks, there is some small amount of information on elements of such a network. Such elements include two paths converging at a network node, and approximately parallel paths separated horizontally.

2.4.5.3.1 Convergent path elements

Information on the diversity improvement factor for converging paths in the low EHF range of the spectrum can be found in Recommendation ITU-R P.1410. Although developed for point-to-area applications, it can be used to give some general indication of the improvement afforded by such elements of a point-to-point route-diversity (or mesh) network, of which there would be two.

2.4.5.3.2 Parallel path elements separated horizontally

Experimental data obtained in the United Kingdom in the 20-40 GHz range give an indication of the improvement in link reliability which can be obtained by the use of parallel-path elements of route-diversity networks. The diversity gain (i.e. the difference between the attenuation (dB) exceeded for a specific percentage of time on a single link and that simultaneously on two parallel links):

– tends to decrease as the path length increases from 12 km for a given percentage of time, and for a given lateral path separation,

– is generally greater for a spacing of 8 km than for 4 km, though an increase to 12 km does not provide further improvement,

– is not significantly dependent on frequency in the range 20-40 GHz, for a given geometry, and

– ranges from about 2.8 dB at 0.1% of the time to 4.0 dB at 0.001% of the time, for a spacing of 8 km, and path lengths of about the same value. Values for a 4 km spacing are about 1.8 to 2.0 dB.

2.4.6 Prediction of outage due to precipitation

In the design of a digital link, calculate the probability, P_{rain}, of exceeding a rain attenuation equal to the flat fade margin F (dB) (see § 2.3.5) for the specified BER from:

$$P_{rain} = p/100 \tag{54}$$

where p (%) is the percentage of time that a rain attenuation of F (dB) is exceeded in the average year by solving equation (42) in § 2.4.1.

3 Variation in angle-of-arrival/launch

Abnormal gradients of the clear-air refractive index along a path can cause considerable variation in the angles of launch and arrival of the transmitted and received waves. This variation is substantially frequency independent and primarily in the vertical plane of the antennas. The range of angles is greater in humid coastal regions than in dry inland areas. No significant variations have been observed during precipitation conditions.

The effect can be important on long paths in which high gain/narrow beam antennas are employed. If the antenna beamwidths are too narrow, the direct outgoing/incoming wave can be sufficiently far off axis that a significant fade can occur (see § 2.3). Furthermore, if antennas are aligned during periods of very abnormal angles-of-arrival, the alignment may not be optimum. Thus, in aligning antennas on critical paths (e.g. long paths in coastal area), it may be desirable to check the alignment several times over a period of a few days.

4 Reduction of XPD

The XPD can deteriorate sufficiently to cause co-channel interference and, to a lesser extent, adjacent channel interference. The reduction in XPD that occurs during both clear-air and precipitation conditions must be taken into account.

4.1 Prediction of outage due to clear-air effects

The combined effect of multipath propagation and the cross-polarization patterns of the antennas governs the reductions in XPD occurring for small percentages of time. To compute the effect of these reductions in link performance the following step-by-step procedures should be used:

Step 1: Compute

$$XPD_0 = \begin{cases} XPD_g + 5 & \text{for } XPD_g \le 35 \\ 40 & \text{for } XPD_g > 35 \end{cases} \tag{55}$$

where XPD_g is the manufacturer's guaranteed minimum XPD at boresight for both the transmitting and receiving antennas, i.e., the minimum of the transmitting and receiving antenna boresight XPDs.

Step 2: Evaluate the multipath activity parameter

$$\eta = 1 - e^{-0.2(P_0)^{0.75}} \tag{56}$$

where $P_0 = p_w/100$ is the multipath occurrence factor corresponding to the percentage of the time p_w (%) of exceeding $A = 0$ dB in the average worst month, as calculated from equation (19).

Step 3: Determine

$$Q = -10 \log\left(\frac{k_{XP}\,\eta}{P_0}\right) \tag{57}$$

where:

$$k_{XP} = \begin{cases} 0.7 & \text{one transmit antenna} \\ 1 - 0.3 \exp\left[-4 \times 10^{-6}\left(\frac{s_t}{\lambda}\right)^2\right] & \text{two transmit antennas} \end{cases} \quad (58)$$

In the case where two orthogonally polarized transmissions are from different antennas, the vertical separation is s_t (m) and the carrier wavelength is λ (m).

Step 4: Derive the parameter C from:

$$C = XPD_0 + Q \quad (59)$$

Step 5: Calculate the probability of outage P_{XP} due to clear-air cross-polarization from:

$$P_{XP} = P_0 \times 10^{-\frac{M_{XPD}}{10}} \quad (60)$$

where M_{XPD} (dB) is the equivalent XPD margin for a reference BER given by:

$$M_{XPD} = \begin{cases} C - \frac{C_0}{I} & \text{without XPIC} \\ C - \frac{C_0}{I} + XPIF & \text{with XPIC} \end{cases} \quad (61)$$

Here, C_0/I is the carrier-to-interference ratio for a reference BER, which can be evaluated either from simulations or from measurements.

XPIF is a laboratory-measured cross-polarization improvement factor that gives the difference in cross-polar isolation (XPI) at sufficiently large carrier-to-noise ratio (typically 35 dB) and at a specific BER for systems with and without cross polar interference canceller (XPIC). A typical value of XPIF is about 20 dB.

4.2 Prediction of outage due to precipitation effects

4.2.1 XPD statistics during precipitation conditions

Intense rain governs the reductions in XPD observed for small percentages of time. For paths on which more detailed predictions or measurements are not available, a rough estimate of the unconditional distribution of XPD can be obtained from a cumulative distribution of the co-polar attenuation (CPA) for rain (see § 2.4) using the equi-probability relation:

$$XPD = U - V(f) \log CPA \quad \text{dB} \quad (62)$$

The coefficients U and $V(f)$ are in general dependent on a number of variables and empirical parameters, including frequency, f. For line-of-sight paths with small elevation angles and horizontal or vertical polarization, these coefficients may be approximated by:

$$U = U_0 + 30 \log f \quad (63)$$

$$\begin{aligned} V(f) &= 12.8\, f^{0.19} && \text{for } 8 \le f \le 20 \text{ GHz} \\ V(f) &= 22.6 && \text{for } 20 < f \le 35 \text{ GHz} \end{aligned} \quad (64)$$

An average value of U_0 of about 15 dB, with a lower bound of 9 dB for all measurements, has been obtained for attenuations greater than 15 dB.

The variability in the values of U and $V(f)$ is such that the difference between the CPA values for vertical and horizontal polarizations is not significant when evaluating XPD. The user is advised to use the value of CPA for circular polarization when working with equation (62).

Long-term XPD statistics obtained at one frequency can be scaled to another frequency using the semi-empirical formula:

$$XPD_2 = XPD_1 - 20 \log (f_2 / f_1) \qquad \text{for } 4 \le f_1,\ f_2 \le 30 \text{ GHz} \tag{65}$$

where XPD_1 and XPD_2 are the XPD values not exceeded for the same percentage of time at frequencies f_1 and f_2.

The relationship between XPD and CPA is influenced by many factors, including the residual antenna XPD, that has not been taken into account. Equation (65) is least accurate for large differences between the respective frequencies. It is most accurate if XPD_1 and XPD_2 correspond to the same polarization (horizontal or vertical).

4.2.2 Step-by-step procedure for predicting outage due to precipitation effects

Step 1: Determine the path attenuation, $A_{0.01}$ (dB), exceeded for 0.01% of the time from equation (41).

Step 2: Determine the equivalent path attenuation, A_p (dB):

$$A_p = 10^{((U - C_0/I + XPIF)/V)} \tag{66}$$

where U is obtained from equation (63) and V from equation (64), C_0/I (dB) is the carrier-to-interference ratio defined for the reference BER without XPIC, and XPIF (dB) is the cross-polarized improvement factor for the reference BER.

If an XPIC device is not used, set XPIF = 0.

Step 3: Determine the following parameters:

$$m = \begin{cases} 23.26 \log \left[A_p / 0.12 A_{0.01} \right] & \text{if } m \le 40 \\ 40 & \text{otherwise} \end{cases} \tag{67}$$

and

$$n = \left(-12.7 + \sqrt{161.23 - 4m} \right) \Big/ 2 \tag{68}$$

Valid values for n must be in the range of –3 to 0. Note that in some cases, especially when an XPIC device is used, values of n less than –3 may be obtained. If this is the case, it should be noted that values of p less than –3 will give outage BER $< 1 \times 10^{-5}$.

Step 4: Determine the outage probability from:

$$P_{XPR} = 10^{(n - 2)} \tag{69}$$

5 Distortion due to propagation effects

The primary cause of distortion on line-of-sight links in the UHF and SHF bands is the frequency dependence of amplitude and group delay during clear-air multipath conditions. In analogue systems, an increase in fade margin will improve the performance since the impact of thermal noise is reduced. In digital systems, however, the use of a larger fade margin will not help if it is the frequency selective fading that causes the performance reduction.

The propagation channel is most often modelled by assuming that the signal follows several paths, or rays, from the transmitter to the receiver. These involve the direct path through the atmosphere and may include one or more additional ground-reflected and/or atmospheric refracted paths. If the direct signal and a significantly delayed replica of near equal amplitude reach the receiver, inter symbol interference occurs that may result in an error in detecting the information. Performance prediction methods make use of such a multi-ray model by integrating the various variables such as delay (time difference between the first arrived ray and the others) and amplitude distributions along with a proper model of equipment elements such as modulators, equalizer, forward-error correction (FEC) schemes, etc. Although many methods exist, they can be grouped into three general classes based on the use of a system signature, linear amplitude

distortion (LAD), or net fade margin. The signature approach often makes use of a laboratory two-ray simulator model, and connects this to other information such as multipath occurrence and link characteristics. The LAD approach estimates the distortion distribution on a given path that would be observed at two frequencies in the radio band and makes use of modulator and equalizer characteristics, etc. Similarly, the net-fade margin approach employs estimated statistical distributions of ray amplitudes as well as equipment information, much as in the LAD approach. In § 5.1, the method recommended for predicting error performance is a signature method.

Distortion resulting from precipitation is believed to be negligible, and in any case a much less significant problem than precipitation attenuation itself. Distortion is known to occur in millimetre and sub-millimetre wave absorption bands, but its effect on operational systems is not yet clear.

5.1 Prediction of outage in unprotected digital systems

The outage probability is here defined as the probability that BER is larger than a given threshold.

Step 1: Calculate the mean time delay from:

$$\tau_m = 0.7 \left(\frac{d}{50} \right)^{1.3} \quad \text{ns} \tag{70}$$

where d is the path length (km).

Step 2: Calculate the multipath activity parameter η as in Step 2 of § 4.1.

Step 3: Calculate the selective outage probability from:

$$P_s = 2.15\eta \left(W_M \times 10^{-B_M/20} \frac{\tau_m^2}{|\tau_{r,M}|} + W_{NM} \times 10^{-B_{NM}/20} \frac{\tau_m^2}{|\tau_{r,NM}|} \right) \tag{71}$$

where:

W_x: signature width (GHz)

B_x: signature depth (dB)

$\tau_{r,x}$: the reference delay (ns) used to obtain the signature, with x denoting either minimum phase (M) or non-minimum phase (NM) fades.

The signature parameter definitions and specification of how to obtain the signature are given in Recommendation ITU-R F.1093.

6 Techniques for alleviating the effects of multipath propagation

The effects of slow relatively non-frequency selective fading (i.e. “flat fading”) due to beam spreading, and faster frequency-selective fading due to multipath propagation can be reduced by both non-diversity and diversity techniques.

6.1 Techniques without diversity

In order to reduce the effects of multipath fading without diversity there are several options that can be employed either if the link is between existing towers or between new towers to be built. The guidance is divided into three groups: reduction of the levels of ground reflection, increase of path inclination, and reduction of path clearance.

6.1.1 Reduction of ground reflection levels

Links should be sited where possible to reduce the level of surface reflections thus reducing the occurrence of multipath fading and distortion. Techniques include the siting of overwater links to place surface reflections on land rather than water and the siting of overland and overwater links to similarly avoid large flat highly reflecting surfaces on land. Another technique known to reduce the level of surface reflections is to tilt the antennas slightly upwards. Detailed

information on appropriate tilt angles is not yet available. A trade-off must be made between the resultant loss in antenna directivity in normal refractive conditions that this technique entails, and the improvement in multipath fading conditions.

6.1.2 Increase of path inclination

Links should be sited to take advantage of terrain in ways that will increase the path inclination, since increasing path inclination is known to reduce the effects of beam spreading, surface multipath fading, and atmospheric multipath fading. The positions of the antennas on the radio link towers should be chosen to give the largest possible inclinations, particular for the longest links.

6.1.3 Reduction of path clearance

Another technique that is less well understood involves the reduction of path clearance. A trade-off must be made between the reduction of the effects of multipath fading and distortion and the increased fading due to sub-refraction. However, for the space diversity configuration (see § 6.2) one antenna might be positioned with low clearance.

6.2 Diversity techniques

Diversity techniques include space, angle and frequency diversity. Frequency diversity should be avoided whenever possible so as to conserve spectrum. Whenever space diversity is used, angle diversity should also be employed by tilting the antennas at different upward angles. Angle diversity can be used in situations in which adequate space diversity is not possible or to reduce tower heights.

The degree of improvement afforded by all of these techniques depends on the extent to which the signals in the diversity branches of the system are uncorrelated. For narrow-band analogue systems, it is sufficient to determine the improvement in the statistics of fade depth at a single frequency. For wideband digital systems, the diversity improvement also depends on the statistics of in-band distortion.

The diversity improvement factor, I, for fade depth, A, is defined by:

$$I = p(A) / p_d(A) \tag{72}$$

where $p_d(A)$ is the percentage of time in the combined diversity signal branch with fade depth larger than A and $p(A)$ is the percentage for the unprotected path. The diversity improvement factor for digital systems is defined by the ratio of the exceedance times for a given BER with and without diversity.

6.2.1 Diversity techniques in analogue systems

The vertical space diversity improvement factor for narrow-band signals on an overland path can be estimated from:

$$I = \left[1 - \exp\left(-3.34 \times 10^{-4} S^{0.87} f^{-0.12} d^{0.48} P_0^{-1.04} \right) \right] 10^{(A - V)/10} \tag{73}$$

where:

$$P_0 = p_w \cdot 10^{A/10}/100 \tag{74}$$

and

$$V = |G_1 - G_2| \tag{75}$$

with:

A: fade depth (dB) for the unprotected path

p_w: percentage of time fade depth A is exceeded in the average worst month

P_0: fading occurrence factor

S: vertical separation (centre-to-centre) of receiving antennas (m)

f: frequency (GHz)

d: path length (km)

G_1, G_2: gains of the two antennas (dBi).

Equation (73) was based on data in the data banks of Radiocommunication Study Group 3 for the following ranges of variables: $43 \le d \le 240$ km, $2 \le f \le 11$ GHz, and $3 \le S \le 23$ m. There is some reason to believe that it may remain reasonably valid for path lengths as small as 25 km. The exceedance percentage p_w can be calculated from equation (19). Equation (73) is valid in the deep-fading range for which equation (19) is valid.

6.2.2 Diversity techniques in digital systems

Methods are available for predicting outage probability and diversity improvement for space, frequency, and angle diversity systems, and for systems employing a combination of space and frequency diversity. The step-by-step procedures are as follows.

6.2.2.1 Prediction of outage using space diversity

In space diversity systems, maximum-power combiners have been used most widely so far. The step-by-step procedure given below applies to systems employing such a combiner. Other combiners, employing a more sophisticated approach using both minimum-distortion and maximum-power dependent on a radio channel evaluation may give somewhat better performance.

Step 1: Calculate the multipath activity factor, η, as in Step 2 of § 4.1.

Step 2: Calculate the square of the non-selective correlation coefficient, k_{ns}, from:

$$k_{ns}^2 = 1 - \frac{I_{ns} \cdot P_{ns}}{\eta} \tag{76}$$

where the improvement, I_{ns}, can be evaluated from equation (73) for a fade depth A (dB) corresponding to the flat fade margin F (dB) (see § 2.3.5) and P_{ns} from equation (36).

Step 3: Calculate the square of the selective correlation coefficient, k_s, from:

$$k_s^2 = \begin{cases} 0.8238 & \text{for} \quad r_w \le 0.5 \\ 1 - 0.195\left(1 - r_w\right)^{0.109 \, - \, 0.13 \log \left(1 \, - \, r_w\right)} & \text{for } 0.5 < r_w \le 0.9628 \\ 1 - 0.3957\left(1 - r_w\right)^{0.5136} & \text{for} \quad r_w > 0.9628 \end{cases} \tag{77}$$

where the correlation coefficient, r_w, of the relative amplitudes is given by:

$$r_w = \begin{cases} 1 - 0.9746\left(1 - k_{ns}^2\right)^{2.170} & \text{for } k_{ns}^2 \le 0.26 \\ 1 - 0.6921\left(1 - k_{ns}^2\right)^{1.034} & \text{for } k_{ns}^2 > 0.26 \end{cases} \tag{78}$$

Step 4: Calculate the non-selective outage probability, P_{dns}, from:

$$P_{dns} = \frac{P_{ns}}{I_{ns}} \tag{79}$$

where P_{ns} is the non-protected outage given by equation (36).

Step 5: Calculate the selective outage probability, P_{ds}, from:

$$P_{ds} = \frac{P_s^2}{\eta\left(1 - k_s^2\right)} \tag{80}$$

where P_s is the non-protected outage given by equation (71).

Step 6: Calculate the total outage probability, P_d, as follows:

$$P_d = \left({P_{ds}}^{0.75} + {P_{dns}}^{0.75}\right)^{1.33} \tag{81}$$

6.2.2.2 Prediction of outage using frequency diversity

The method given applies for a 1 + 1 system. Employ the same procedure as for space diversity, but in Step 2 use instead:

$$I_{ns} = \frac{80}{fd}\left(\frac{\Delta f}{f}\right)10^{F/10} \tag{82}$$

where:

Δf: frequency separation (GHz). If $\Delta f > 0.5$ GHz, use $\Delta f = 0.5$

f: carrier frequency (GHz)

F: flat fade margin (dB).

6.2.2.3 Prediction of outage using angle diversity

Step 1: Estimate the average angle of arrival, μ_θ, from:

$$\mu_\theta = 2.89 \times 10^{-5}\ G_m\ d \qquad \text{degrees} \tag{83}$$

where G_m is the average value of the refractivity gradient (N-unit/km). When a strong ground reflection is clearly present, μ_θ can be estimated from the angle of arrival of the reflected ray in standard propagation conditions.

Step 2: Calculate the non-selective reduction parameter, r, from:

$$r = \begin{cases} 0.113 \sin\left[150\,(\delta/\Omega) + 30\right] + 0.963 & \text{for } q > 1 \\ q & \text{for } q \le 1 \end{cases} \tag{84}$$

where:

$$q = 2\,505 \times 0.0437^{(\delta/\Omega)} \times 0.593^{(\varepsilon/\delta)} \tag{85}$$

and

δ: angular separation between the two patterns

ε: elevation angle of the upper antenna (positive towards ground)

Ω: half-power beamwidth of the antenna patterns.

Step 3: Calculate the non-selective correlation parameter, Q_0, from:

$$Q_0 = r\left(0.9399^{\mu_\theta} \times 10^{-24.58\,\mu_\theta^2}\right)\left[2.469^{1.879^{(\delta/\Omega)}} \times 3.615^{\left[(\delta/\Omega)^{1.978}(\varepsilon/\delta)\right]} \times 4.601^{\left[(\delta/\Omega)^{2.152}(\varepsilon/\delta)^2\right]}\right] \tag{86}$$

Step 4: Calculate the multipath activity parameter, η, as in Step 2 of § 4.1.

Step 5: Calculate the non-selective outage probability from:

$$P_{dns} = \eta\ Q_0 \times 10^{-F/6.6} \tag{87}$$

Step 6: Calculate the square of the selective correlation coefficient, k_s, from:

$$k_s^2 = 1 - \left(0.0763 \times 0.694^{\mu_\theta} \times 10^{23.3\,\mu_\theta^2}\right)\delta\left(0.211 - 0.188\,\mu_\theta - 0.638\,\mu_\theta^2\right)^{\Omega} \tag{88}$$

Step 7: The selective outage probability, P_{ds}, is found from:

$$P_{ds} = \frac{P_s^2}{\eta\left(1 - k_s^2\right)} \tag{89}$$

where P_s is the non-protected outage (see Step 3 of § 5.1).

Step 8: Finally, calculate the total outage probability, P_d, from:

$$P_d = \left(P_{ds}^{0.75} + P_{dns}^{0.75} \right)^{1.33} \quad (90)$$

6.2.2.4 Prediction of outage using space and frequency diversity (two receivers)

Step 1: The non-selective correlation coefficient, k_{ns}, is found from:

$$k_{ns} = k_{ns,s} \; k_{ns,f} \quad (91)$$

where $k_{ns,s}$ and $k_{ns,f}$ are the non-selective correlation coefficients computed for space diversity (see § 6.2.2.1) and frequency diversity (see § 6.2.2.2), respectively.

The next steps are the same as those for space diversity.

6.2.2.5 Prediction of outage using space and frequency diversity (four receivers)

Step 1: Calculate η as in Step 2 of § 4.1.

Step 2: Calculate the diversity parameter, m_{ns}, as follows:

$$m_{ns} = \eta^3 \left(1 - k_{ns,s}^2 \right) \left(1 - k_{ns,f}^2 \right) \quad (92)$$

where $k_{ns,s}$ and $k_{ns,f}$ are obtained as in § 6.2.2.4.

Step 3: Calculate the non-selective outage probability, P_{dns}, from:

$$P_{dns} = \frac{P_{ns}^4}{m_{ns}} \quad (93)$$

where P_{ns} is obtained from equation (36).

Step 4: Calculate the square of the equivalent non-selective correlation coefficient, k_{ns}, from:

$$k_{ns}^2 = 1 - \sqrt{\eta} \left(1 - k_{ns,s}^2 \right) \left(1 - k_{ns,f}^2 \right) \quad (94)$$

Step 5: Calculate the equivalent selective correlation coefficient, k_s, using the same procedure as for space diversity (Step 3).

Step 6: The selective outage probability, P_{ds}, is found from:

$$P_{ds} = \left[\frac{P_s^2}{\eta \left(1 - k_s^2 \right)} \right]^2 \quad (95)$$

where P_s is the non-protected outage given by equation (71).

Step 7: The total outage probability, P_d, is then found from equation (81).

7 Prediction of total outage

Calculate the total outage probability due to clear-air effects from:

$$P_t = \begin{cases} P_{ns} + P_s + P_{XP} & \\ P_d + P_{XP} & \text{if diversity is used} \end{cases} \quad (96)$$

obtained by methods given in § 2.3.5, 4.1, 5.1, and 6.2.2.

The total outage probability due to rain is calculated from taking the larger of P_{rain} and P_{XPR} obtained by methods given in § 2.4.6 and 4.2.2.

The outage prediction methods given for digital radio systems have been developed from a definition of outage as BER above a given value (e.g. 1×10^{-3}) for meeting requirements set out in ITU-T Recommendation G.821. The outage is apportioned to error performance and availability (see Recommendations ITU-R F.594, ITU-R F.634, ITU-R F.695, ITU-R F.696, ITU-R F.697, ITU-R F.1092, ITU-R F.1189 and ITU-R F.557). The outage due to clear-air effects is apportioned mostly to performance and the outage due to precipitation, predominantly to availability. However, it is likely that there will be contributions to availability from clear-air effects and contributions to performance from precipitation.

If requirements in ITU-T Recommendation G.826 have to be met there is a need for prediction methods that are based on estimating block errors rather than bit errors. In order to meet the requirements in ITU-T Recommendation G.826 the link should be designed using the methods given in Annex 2.

APPENDIX 1

TO ANNEX 1

Method for determining the geoclimatic factor, *K*, from measured overland fading data

Step 1: Obtain the worst calendar month envelope fading distribution for each year of operation, using the long-term median value as a reference. Average these to obtain the cumulative fading distribution for the average worst month and plot this on a semi-logarithmic graph.

Step 2: From the graph note the fade depth, A_1, beyond which the cumulative distribution is approximately linear and obtain the corresponding percentage of time, p_1. This linear portion constitutes the large fade depth tail which can vary by up to about 3 or 4 dB/decade in slope about the average "Rayleigh" value of 10 dB/decade, the amount of this variation depending on the number of years of data contained in the average distribution.

Step 3: Calculate the path inclination $|\varepsilon_p|$ from equation (18).

Step 4: Substitute the coordinates (p_1, A_1) of the "first tail point" into equation (19) along with the values d, f, $|\varepsilon_p|$ and calculate the geoclimatic factor, K.

Step 5: If data are available for several paths in a region of similar climate and terrain, or several frequencies, etc., on a single path, an average geoclimatic factor should be obtained by averaging the values of log K.

ANNEX 2

Prediction of error performance and availability of line-of-sight synchronous digital hierarchy radio links

1 Introduction

Synchronous digital hierarchy (SDH) networks, or synchronous optical networks (SONET), currently allow radio link systems with capacities in synchronous transfer mode from 51 Mbit/s (STM-0) to 622 Mbit/s (STM-4). International Recommendations and Standards define the error performance and availability objectives for SDH networks. These objectives are media independent, and still have to be met whenever radio forms a part of the network.

The prediction methods given in this Annex are based on a theoretically-derived relationship between BER and the new SDH parameters based on errored blocks (EB). The methods take into account system characteristics such as burst errors along with the parameters needed for predicting the outage time based on BER.

2 Error performance and availability objectives

ITU-T Recommendations G.826 and G.827 give the requirements for error performance and availability, respectively. Since these Recommendations give the end-to-end objectives, other Recommendations are needed when dealing with actual radio links. In order to apportion the allowances to individual paths with actual hop lengths, operating radio frequency, etc., a number of additional Recommendations have therefore been issued dealing with radio as an SDH network element.

2.1 Error performance and availability parameters

ITU-T Recommendation G.826 defines a set of block-based error performance events and parameters devoted to in-service error performance monitoring of an SDH path (see Note 1). An EB is one in which one or more bits are in error. An errored second (ES) occurs if there are one or more errored blocks on at least one defect such as a loss of pointer (LOP). A severely errored second (SES) occurs if there are 30% or more of EBs or a defect. Background block error (BBE) is an errored block not occurring as part of an SES. Parameters defined are severely errored second ratio (SESR), background block error ratio (BBER), and errored second ratio (ESR).

NOTE 1 – An SDH path is a trail carrying an SDH payload and associated overhead through the layered transport network between the path terminating equipment. A digital path may be bidirectional or unidirectional and may comprise both customer-owned portions and network-operator-owned portions (for more information see ITU-T Recommendations G.803, G.805, G.828).

The definition of block size and of error performance events for SDH multiplex section (MS) and regenerator section (RS) are presented in ITU-T Recommendation G.829, while the error performance parameters and objectives for SDH MS and RS on an individual digital radio-relay hop, are being developed for the ITU-R F Series of Recommendations.

Each direction of a path can be in one of two states, available time or unavailable time. The criteria determining the transition between the two states are as follows: A period of unavailable time begins at the onset of 10 consecutive SES events. These 10 s are considered to be part of unavailable time. A new period of available time begins at the onset of 10 consecutive non-SES events. These 10 s are considered to be part of available time. A path is available if, and only if, both directions are available.

The availability parameters defined are: availability ratio (AR) and mean time between digital path outage *Mo*. The converse of AR is the unavailability ratio (UR). Thus, $AR + UR = 1$. The reciprocal of *Mo* is defined as the outage intensity (OI). Thus, $Mo = 1/OI$. *Mo* is regarded as the number of unavailable periods per year.

NOTE 2 – The threshold of 30% EB*s* is defined for SDH path in ITU-T Recommendation G.826, while for SDH MS and RS the threshold value is defined in ITU-T Recommendation G.829.

2.2 Objectives for digital radio-relay digital paths

The error performance objectives given for digital paths at or above the primary rate (2.048 or 1.544 Mbit/s) are different for national and international portions. The specified objectives must be met for any month. ITU-R has adopted objectives for both national (see Recommendation ITU-R F.1189) and international (see Recommendation ITU-R F.1092) paths. For the national portion there is a subdivision into three sections. These are: long haul, short haul and access network sections. The allocation of the error performance objectives for the short haul and access sections shall each make use of a fixed block allocation in the range of 7.5% to 8.5% of the end-to-end objectives. The allocation of the objectives for the long haul section shall make use of a distance based allocation per 500 km and a fixed block allocation in the range of 1% to 2% of the end-to-end objectives. In these Recommendations there is no indication on apportioning for individual radio hops. However, Radiocommunication Study Group 9 is developing new Recommendations for apportioning these objectives to links consisting of one or more radio hops.

The availability objectives are defined in ITU-T Recommendation G.827. However, ITU-R has used the objective of 99.7% available time of a year for a 2 500 km reference path (see Recommendation ITU-R F.557). The unavailable time of 0.3% is divided linearly (per km) on the individual high grade links (see Recommendation ITU-R F.695) covering 280 to 2 500 km, with 0.033% for the remaining 280 km. Furthermore new availability guidelines are being developed for the ITU-R F Series of Recommendations for a link forming part of an SDH path at or above the primary rate.

3 Predicting error performance and availability

The relationship between the error performance parameters and BER is evaluated employing both random (Poisson) and burst error (Neyman-A) distributions. Modern radio transmission systems, which implement complex modulation schemes, error correction codes, equalizers, etc., tend to produce clusters or bursts of errors (see Note 1). Typical values for high level modulation (e.g. 128-trellis code modulation (128-TCM)) are 10 to 20 errors per burst.

NOTE 1 – A burst of errors is defined as a sequence of errors which starts and ends with an errored bit such that the time between two errors is less than the memory of the system (e.g., the constraint length of the convolutional code, the code size for block code, etc).

The new SDH prediction methods are based on theoretical assumptions relating BER, which is the fundamental parameter of existing prediction methods, to the error performance parameters ESR, SESR and BBER. Since the methods are based on BER they automatically cover both multipath and attenuation due to rain. In the following paragraphs some background information is given followed by step-by-step calculation procedures.

3.1 Prediction of SESR

The procedure for predicting SESR is based on the relationship between SESR and BER, where the methods for predicting outage defined by a specified BER are given in Annex 1. Generally the SESR is predicted by:

$$SESR = \int_{BER_A}^{BER_B} f_{SES}(x) \quad g_{BER}(x)\ \mathrm{d}x \tag{97}$$

where $f_{SES}(x)$ represents the relationship between SES and the BER, $g_{BER}(x)$ is the probability density function (PDF) of BER, and BER_A and BER_B are the integration limits (typical values are 1×10^{-9} and 1×10^{-3}).

3.1.1 Prediction of SESR due to multipath propagation effects

The SESR parameter is given by equation (97) where the second term is the PDF of BER. In the case of multipath propagation, the BER is strictly connected to the outage probability P_t, evaluated by the methods in Annex 1. Using appropriate methods for the transmission system considered, the outage probability P_t versus BER can be derived (e.g. see Fig. 7). The function g_{BER} is derived from Fig. 7, i.e. $g_{BER} = \mathrm{d}P_t/\mathrm{d}BER$.

In general, the values of outage probability are obtained for only a few values of BER where equipment signature and threshold are known. If an extended set of BER values are available, a more precise curve can be obtained.

The SESR evaluation is made in two steps, one to determine the amount of SES due to EB, and a second one to obtain the usually negligible part corresponding to LOP.

The curve of SESR due to EB can be approximated by a step function. The BER value, where the SES probability changes from 0 to 1 is denoted BER_{SES}.

$$f_{SES}(x) = \begin{cases} 0 & \text{for } BER < BER_{SES} \\ 1 & \text{for } BER \geq BER_{SES} \end{cases} \tag{98}$$

FIGURE 7

Outage probability, P_t, versus BER due to multipath propagation

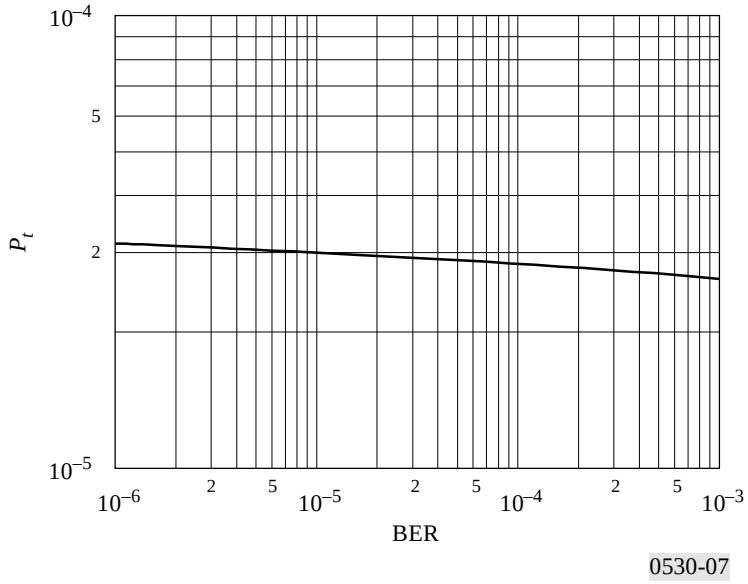

The value of BER_{SES} normalized to the mean number of errors per bursts m ($m = 1$ for Poisson distribution) is given in Table 2.

TABLE 2

***BER*$_{SES}$ for various SDH paths and MS sections**

Path type	Bit rate supported (Mbit/s)	BER_{SES} (Notes 1 and 2)	Blocks/s, n (Note 2)	Bits/block, N_B (Note 2)
VC-11	1.5	$5.4 \times 10^{-4}\ \alpha$	2 000	832
VC-12	2	$4.0 \times 10^{-4}\ \alpha$	2 000	1 120
VC-2	6	$1.3 \times 10^{-4}\ \alpha$	2 000	3 424
VC-3	34	$6.5 \times 10^{-5}\ \alpha$	8 000	6 120
VC-4	140	$2.1 \times 10^{-5}\ \alpha$	8 000	18 792
STM-1	155	$2.3 \times 10^{-5}\ \alpha$ $1.3 \times 10^{-5}\ \alpha + 2.2 \times 10^{-4}$	8 000 192 000	19 940 801

NOTE 1 – $\alpha = 1$ indicates a Poisson distribution of errors.

NOTE 2 – The blocks/s are defined in ITU-T Recommendation G.826 for SDH path, in ITU-T Recommendation G.829 for SDH sections. Some STM-1 equipment might be designed with 8 000 blocks/s (19 940 bits/block), but ITU-T Recommendation G.829 defines the block rate and size to be 192 000 blocks/s and 801 bits/block, respectively.

Considering equation (98), in the case of SES due to EB, equation (97) becomes:

$$SESR = \int_{BER_A}^{BER_B} f_{SES}(x)\ \ g_{BER}(x)\ \mathrm{d}x = P_t(BER_{SES}) \tag{99}$$

Upper limit for SES due to LOP

To evaluate the upper limit, $SESR_{LOPu}$, it is supposed that the probability of SES for BER values less than BER_{SES} is a constant. Then,

$$SESR_{LOPu} = P\left(SES \mid BER = BER_{SES}\right)\left(1 - P_t\left(BER_{SES}\right)\right) \quad (100)$$

NOTE – The contribution from LOP has been found to be small, and can therefore be ignored.

Step-by-step procedure for calculation of SES due to multipath

Step 1: Calculate the outage probability P_{tSES} for $BER = BER_{SES}$ for the appropriate system, using the outage prediction methods described in Annex 1.

$$SESR = P_{tSES} = P_t(BER_{SES}) \quad (101)$$

where BER_{SES} is given in Table 2.

3.1.2 Prediction of SESR due to rain

Rain may introduce severe attenuation. Most of the time X% when rain attenuation exceeds the threshold A_1, an unavailability condition will occur. The remaining time $100 - X\% = Y\%$ is considered as available time giving rise to SES. The division between available and unavailable time for any climatic region has to be found from experimental measurements.

The process of obtaining the SESR due to rain implies finding the attenuation margin of the radio link for a BER, BER_{SES}, where all seconds are SES. Then it is possible to evaluate the percentage of time in the worst month that the rain attenuation exceeds this margin, and finally to evaluate the corresponding annual percentage of time. The SESR value due to rain will be Y% of this probability.

3.1.2.1 Step-by-step procedure for calculation of SESR due to rain

In the following, a step-by-step procedure for evaluating SESR due to rain is given. The input parameters are: frequency, hop length, polarization, rain zone, transmission power, gain of transmitting antenna, gain of receiving antenna, relationship between received power and BER, SDH path type, and error burst length.

Step 1: Calculate the rain attenuation exceeded for 0.01% of time, $A_{0.01}$, using the method in § 2.4.1 of Annex 1.

Step 2: Calculate the nominal received power without rain attenuation, $P_{RXnominal}$.

Step 3: Using the relationship between the received power and BER (usually obtained from equipment manufacturers) obtain the value of A_{SES}, where A_{SES} is the attenuation margin of the radio link for $BER = BER_{SES}$ (see Table 2).

Step 4: Calculate the annual time percentage, p_{aSES}, that the rain attenuation is larger than A_{SES}, using the method in § 2.4.1 of Annex 1.

Step 5: Translate the annual time percentage, p_{aSES}, to worst-month percentage, p_{wSES}, using the method in Recommendation ITU-R P.841.

Step 6: Calculate SESR from:

$$SESR = Y(\%)\, P_{wSES} \quad (102)$$

where P_{wSES} is the worst-month probability ($P_{wSES} = p_{wSES} / 100$).

NOTE 1 – The value of X is under study; for the time being $Y = 0\%$ is suggested.

3.2 Prediction of BBER

The BBER is evaluated for multipath and rain conditions from:

$$BBER = \int_{BER_A}^{BER_B} f_{BBER}(x) \quad g_{BER}(x)\ \mathrm{d}x \tag{103}$$

where $f_{BBER}(x)$ represents the relationship between BBER and BER, $g_{BER}(x)$ represents the PDF of BER, and BER_A and BER_B, are the integration limits (typical values are 1×10^{-12} and 1×10^{-3}).

3.2.1 Prediction of BBER due to multipath

Two alternative methods can be used: a complete one based on the analytical solution of the integral in equation (103), where $g_{BER}(x)$ is derived from the outage prediction model (Fig. 7) and $f_{BBER}(x)$ is the theoretical relationship for *BBER* due to *BER*, and a simplified method based on approximation of $f_{BBER}(x)$ and of $g_{BER}(x)$.

3.2.1.1 Step-by-step procedure for BBER due to multipath

In this section a step-by-step procedure based on the simplified prediction model is given.

Step 1: Calculate the outage probability, P_{tR}, for the residual BER (RBER) (typically in the range from 1×10^{-10} to 1×10^{-13} for the bit rates of 2 to 155 Mbit/s, respectively), using the outage prediction methods described in Annex 1 for the appropriate system:

$$P_{tR} = P_t(RBER) \tag{104}$$

Step 2: Calculate the outage probability at $BER = BER_{SES}$ as in the previous step:

$$P_{tSES} = P_t(BER_{SES}) \tag{105}$$

BER_{SES} is given in Table 2.

Step 3: Calculate the SESR as in Step 1 for multipath (see § 3.1.1):

$$SESR = P_{tSES} = P_t(BER_{SES}) \tag{106}$$

Step 4: Calculate the BBER from:

$$BBER = SESR \frac{\alpha_1}{2.8\,\alpha_2(m - 1)} + \frac{N_B\ RBER}{\alpha_3} \tag{107}$$

where:

α_1 = 10 to 30, number of errors per burst for the BER in the range from 1×10^{-3} to BER_{SES}

α_2 = 1 to 10, number of errors per burst for the BER in the range from BER_{SES} to RBER

α_3 = 1, number of errors per burst for the BER lower than RBER

N_B: number of bits/block (see Table 2)

m: slope of the BER distribution curve on a log-log scale for BER in the range from BER_{SES} to RBER, given by:

$$m = \frac{\log_{10}(RBER) - \log_{10}(BER_{SES})}{\log_{10}(P_{tR}) - \log_{10}(P_{tSES})} \tag{108}$$

3.2.2 Prediction of BBER due to rain

The prediction model for BBER due to rain is based on the relationship between the ITU-R rain attenuation model and the BER versus *C/N* ratio of the transmission system being considered.

3.2.2.1 Step-by-step procedure for BBER due to rain

The input parameters are: frequency, hop length, polarization, rain zone, transmission power, gain of transmitting antenna, gain of receiving antenna, relationship between received power and BER, SDH path type, and error burst length.

Step 1: Calculate the rain attenuation exceeded for 0.01% of time, $A_{0.01}$, using the method in § 2.4.1 of Annex 1.

Step 2: Calculate the nominal received power without rain attenuation, $P_{RXnominal}$.

Step 3: Using the relationship between received power and BER (usually obtained from equipment manufacturers) obtain the value of A_{SES}, where A_{SES} is the attenuation margin of the radio link for $BER = BER_{SES}$ (see Table 2).

Step 4: Calculate the annual time percentage, p_{aSES}, that the rain attenuation is larger than A_{SES}, using the method in § 2.4.1 of Annex 1.

Step 5: Translate the annual time percentage p_{aSES} to worst-month percentage, p_{wSES}, using the method in Recommendation ITU-R P.841.

Step 6: Using the relationship between received power and BER (usually obtained from equipment manufacturers) obtain the value of A_R, where A_R is the attenuation margin of the radio link for RBER).

Step 7: Calculate the annual time percentage, p_{aR}, that the rain attenuation is larger than A_R, using the method in § 2.4.1 of Annex 1.

Step 8: Translate the annual time percentage, p_{aR}, to worst-month percentage, p_w, using the method in Recommendation ITU-R P.841.

Step 9: Transform the worst-month percentages, p_{wSES}, and p_{wR}, into the corresponding probabilities, P_{wSES} and P_{wR}.

Step 10: Calculate BBER from:

$$BBER = SESR \frac{\alpha_1}{2.8\,\alpha_2 (m - 1)} + \frac{N_B\ RBER}{\alpha_3} \tag{109}$$

where:

$$\alpha_1 / \alpha_2 \lesssim 2$$

and

α_1 = 1 to 30, number of errors per burst for the BER in the range from 1×10^{-3} to BER_{SES}

α_2 = 1 to 20, number of errors per burst when the BER is in the range from BER_{SES} to RBER

α_3 = 1, number of errors per burst for the BER equal to or lower than RBER

N_B: number of bits/block (see Table 2)

m: slope of the BER distribution curve on a log-log scale for BER in the range from BER_{SES} to RBER given by:

$$m = \frac{\log_{10}(RBER) - \log_{10}(BER_{SES})}{\log_{10}(P_{wR}) - \log_{10}(P_{wSES})} \tag{110}$$

3.3 Prediction of ESR

The ESR is evaluated for multipath and rain conditions from:

$$ESR = \int_{BER_A}^{BER_B} f_{ESR}(x)\ \ g_{BER}(x)\ \mathrm{d}x \tag{111}$$

where $f_{ESR}(x)$ represents the relationship between ESR and BER, $g_{BER}(x)$ is the PDF of BER, and BER_A and BER_B the integration limits (typical values are 1×10^{-12} and 1×10^{-3}).

3.3.1 Prediction of ESR parameter due to multipath

In this section a step-by-step procedure based on an approximation for the integral (equation (111)) is presented.

Step 1: Calculate the outage probability, P_{tR}, for the RBER, using the outage prediction methods described in Annex 1 for the appropriate system:

$$P_{tR} = P_t(RBER) \tag{112}$$

Step 2: Calculate the outage probability at $BER = BER_{SES}$ as in the previous step:

$$P_{tSES} = P_t(BER_{SES}) \tag{113}$$

where BER_{SES} is given in Table 2.

Step 3: Calculate SESR from:

$$SESR = P_{tSES} = P_t(BER_{SES}) \tag{114}$$

Step 4: Calculate ESR from:

$$ESR = SESR \sqrt[m]{n} + \frac{n\, N_B\ RBER}{\alpha_3} \tag{115}$$

where:

α_3 = 1, number of errors per burst for BER lower than RBER

N_B: number of bits/block (see Table 2)

n: number of blocks/s (see Table 2)

m: slope of the BER distribution curve on a log-log scale for BER in the range from BER_{SES} to RBER, given by:

$$m_2 = \frac{\log_{10}(RBER) - \log_{10}(BER_{SES})}{\log_{10}(P_{tR}) - \log_{10}(P_{tSES})} \tag{116}$$

3.3.2 Prediction of ESR parameter due to rain attenuation

The prediction model for BBER due to rain is based on the relationship between the ITU-R rain attenuation model and the BER versus *C/N* ratio of the transmission system being considered.

The input parameters are: frequency, hop length, polarization, rain zone, transmission power, gain of transmitting antenna, gain of receiving antenna, relationship between received power and BER, SDH path type, error burst length.

Step 1: Calculate the rain attenuation exceeded for 0.01% of time, $A_{0.01}$, using the method in Annex 1.

Step 2: Calculate the nominal received power without rain attenuation, $P_{RXnominal}$.

Step 3: Using the relationship between received power and BER (usually obtained from equipment manufacturers) obtain the value of A_{SES}, where A_{SES} is the attenuation margin of the radio link for $BER = BER_{SES}$ (see Table 2).

Step 4: Calculate the annual time percentage, p_{aSES}, that the rain attenuation is larger than A_{SES} using Annex 1.

Step 5: Translate the annual time percentage, p_{aSES}, to the worst-month percentage, p_{wSES}, using the method in Recommendation ITU-R P.841.

Step 6: Using the relationship between received power and BER (usually obtained from equipment manufacturers) obtain the value of A_R, where A_R is the attenuation margin of the radio link for RBER.

Step 7: Calculate the annual time percentage, p_{aR}, that the rain attenuation is larger than A_R using Annex 1.

Step 8: Translate the annual time percentage, p_{aR}, into worst-month percentage, p_{wR}, using the method in Recommendation ITU-R P.841.

Step 9: Transform the worst-month percentages, p_{wSES} and p_{wR}, into the corresponding probabilities, P_{wSES} and P_{wR}:

$$ESR = SESR \sqrt[m]{n} + \frac{n N_B \ RBER}{\alpha_3} \tag{117}$$

where:

α_3 = 1, number of errors per burst, for BER lower than RBER

N_B: number of bits/block (see Table 2)

n: number of blocks/s (see Table 2)

m: slope of the BER distribution curve on a log-log scale for BER in the range from BER_{SES} to RBER, given by:

$$m = \frac{\log_{10}(RBER) - \log_{10}(BER_{SES})}{\log_{10}(P_{wR}) - \log_{10}(P_{wSES})} \tag{118}$$

3.4 Prediction of unavailability

According to the current definition, the unavailability is caused by long SES periods. A radio system is either in the available state or in the unavailable state. If the system is in an available state, and a period of SES occurs that is longer than 10 consecutive seconds, the system will change to an unavailable state, and the period of SES becomes unavailable time. If the system is in an unavailable state, the requirement for changing to available state is a period of 10 consecutive seconds with non-SES. At the moment, it is assumed that it is only fades due to rain that cause unavailable time. It is therefore straightforward to calculate unavailability by using the method for SESR due to rain (see § 3.1.2).